Supplement of Atmos. Chem. Phys., 17, 501–520, 2017
http://www.atmos-chem-phys.net/17/501/2017/
doi:10.5194/acp-17-501-2017-supplement


Atmospheric Chemistry and Physics Open Access EGU

*Supplement of*

# Quantifying the volatility of organic aerosol in the southeastern US

**Provat K. Saha et al.**

*Correspondence to:* Andrew P. Grieshop (apgriesh@ncsu.edu)

**S1. Estimation of approximate equivalent OA MFR for VRT-TD/SMPS data**

We assumed that measured total volume of submicron aerosol ($V_{tot}$) by SMPS (10-600 nm) is comprised of the volume of organic ($V_{org}$) and ammonium sulfate ($V_{as}$). Since the sample was sufficiently dried (RH < 30-40%) before traveling to instruments, the contribution of water to $V_{tot}$ was neglected. Contributions of nitrate and chloride aerosol were also neglected.

$$V_{tot} = V_{org} + V_{as} \tag{S-1}$$

Apply the mass-volume relationship, the mass of organic aerosol ($m_{org}$) can be written as

$$m_{org} = \left( V_{tot} - \frac{m_{as}}{\rho_{as}} \right) \rho_{org} \tag{S-2}$$

Where, $\rho_{org}$ and $\rho_{as}$ are the densities of organic aerosol and ammonium sulfate aerosol, respectively.

Organic aerosol mass fraction remaining (OA MFR) at a TD temperature and residence time (T, Rt) is

$$MFR_{org}\ (T,\ \mathrm{Rt}) = \frac{m_{org,\ TD\ (T,Rt)}}{m_{org,\ BP}} \tag{S-3}$$

Where, 'TD' refers to thermodenuder and 'BP' for bypass.

Replacing $m_{org}$ in Eq.S3 with Eq. S2

$$MFR_{org}(T,\ \mathrm{Rt}) = \frac{\left( V_{tot,\ TD(T,\ \mathrm{Rt})} - \frac{m_{as,\ TD(T,Rt)}}{\rho_{as}} \right) \rho_{org,\ TD(T,Rt)}}{\left( V_{tot,\ BP} - \frac{m_{as,\ BP}}{\rho_{as}} \right) \rho_{org,\ BP}} \tag{S-4}$$

Here, $V_{tot}$ is in $\mu m^3\ cm^{-3}$ and mass of ammonium sulfate ($m_{as}$) is in $\mu g\ m^{-3}$. $\rho_{as}$ is considered 1.77 gm $cm^{-3}$. Change in $\rho_{org}$ after heating at moderate temperature (<100˚C) is assumed to be small ($\rho_{org,BP} \sim \rho_{org,TD}$). It is assumed that ammonium sulfate did not evaporate at a TD temperature < 100˚C ($m_{as,BP} \sim m_{as,TD}$). Note, in MFR calculation, particle loss in TD due to diffusional and inertial and thermophoresis deposition were applied separately via empirically estimated correction factors as a function of temperature and residence time (Saha et al., 2015). Relative transmission of $V_{tot}$ and different aerosol species (e.g., organic, sulfate, nitrate, and ammonium) are assumed to be the same.

To estimate mass of ammonium sulfate mass ($m_{as}$), we assumed a stoichiometric relationship between sulfate and ammonium. Therefore, $m_{as}$ is calculated as $\frac{132}{96} \times m_{SO4;} \sim 1.375 \times m_{SO4.}$

$$MFR_{org}(T,Rt)=\frac{\left(V_{tot,\ TD\ (T,\ Rt)}-\frac{1.375\times m_{SO_4,\ BP}}{\rho_{as}}\right)}{\left(V_{tot,\ BP}-\frac{1.375\times m_{SO_4,\ BP)}}{\rho_{as}}\right)} \quad \text{(S-5)}$$

Eq.S-5 was applied to estimate an approximate OA MFR for VRT-TD data at 60 ˚C and 90˚C, where $m_{SO4,\ BP}$ is used from ACSM measurements.

In Eq. S-5, contribution of ammonium nitrate (AN) aerosol to $V_{tot}$ is neglected, which has a relatively minor influence on the estimated OA MFR at both of our measurement sites. This is because the overall contribution of AN in $PM_1$ was small (Fig. S6). The observed evaporation of ambient AN aerosol is much less than the laboratory generated pure AN aerosol (Huffman et al., 2009) and its observed evaporation is quite similar to the OA evaporation (Fig. S2). Since evaporation of AN under VRT-TD operating conditions would be a function of temperature and residence time, an exclusion of contribution of AN from $V_{tot}$ is not as straightforward as for AS. However, we explore the overall influences of AN on the estimated OA MFR by examining an extreme case. In this analysis, we considered the Raleigh data set, where relatively more $NO_3$ contribution in $PM_1$ was measured (Fig. S6, S7) and the highest operating Rt of VRT-TD (40 s), where maximum bias is expected. Estimated OA MFR using Eq. S-5 (neglecting AN contribution) at 60 ˚C and Rt = 40 s was 0.72 ± 0.06 (base case). In a sensitivity case, we included the contribution of AN ($V_{tot}= V_{org}+V_{as}+V_{an}$) and assumed that evaporation of $NO_3$ measured in TS-TD (60˚C, Rt = 50 s) is same in VRT-TD for the above condition. The estimated mean OA MFR from sensitivity case was 0.735, which is within ~ 2% of our base case estimation and falls well within the variability range. At 90 ˚C and Rt = 40 s, estimated mean OA MFR in sensitivity case was 0.498 versus 0.48 ± 0.078 in base case, which is within 4 %.

**S2. Estimation of condensation sink diameter ($d_{cs}$)**

The condensation sink diameter is estimated following Lehtinen et al., 2003. The condensation sink diameter is the diameter where a monodisperse population of particles of number concentration $N_{tot}$ can be placed to obtain the same total condensation sink (CS) as for a poly-disperse distribution of particles with total number concentration $N_{tot}$ (Lehtinen et al., 2003).

Mathematically, $2\pi D d_{cs} F(d_{cs}) N_{tot} = 2\pi D \sum F\left(d_{p,i}\right) d_{p,i} N_i = CS$ (S-6)

Where, D is the diffusion coefficient, F is the Fuchs and Sutugin correction factor, $N_i$ is the number concentration of particles in size bin of $d_{p,i}$

## S3. Supplementary Figures

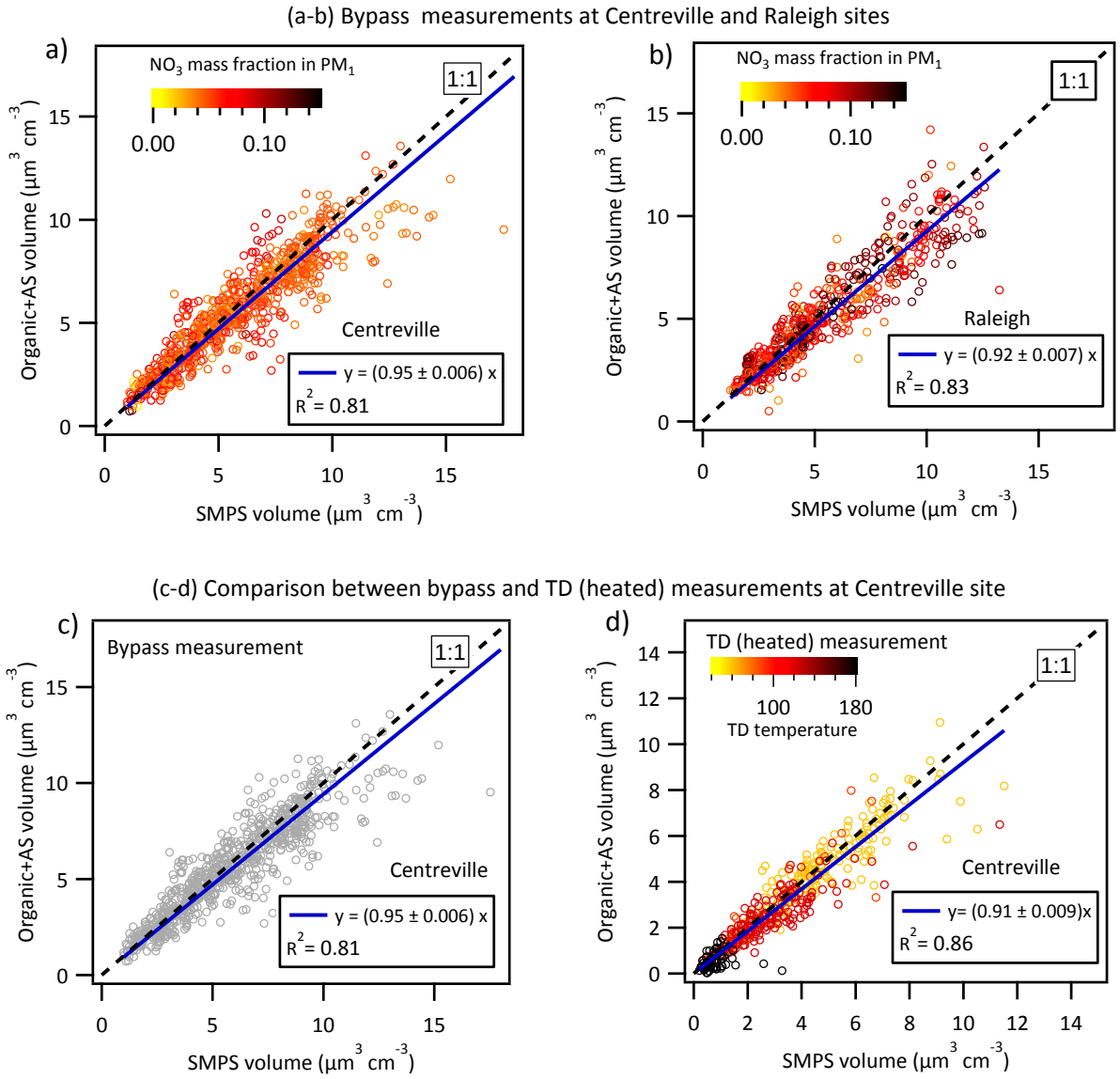


**Figure S1:** Comparison of submicron ambient aerosol volume concentrations measured by SMPS (10-600 nm) with the volume concentrations of organic aerosol (OA) + ammonium sulfate (AS) aerosol measured by ACSM. Both bypass and TD (heated) ACSM data were analyzed using a collection efficiency (CE) of 0.5 (Ng et al., 2011a) for all species. OA volume are calculated from the measured OA mass concentrations ($m_{org}$) and an effective density of OA of 1.4 g cm$^{-3}$ , estimated from a parameterization using elemental composition (O:C; H:C) (Kuwata et al., 2012). AS mass concentration ($m_{as}$) is calculated as $\frac{132}{96} \times m_{SO4}$ , where $m_{SO4}$ is the mass concentration of sulfate ($SO_4$). AS volume is calculated assuming density of 1.77 g cm$^{-3}$.

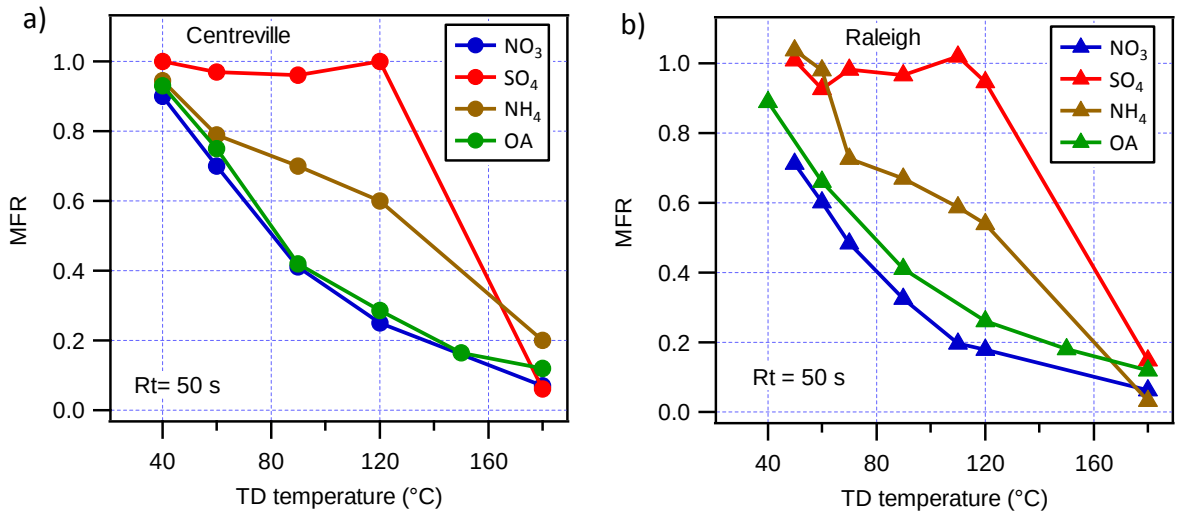


**Figure S2:** Campaign average mass thermogram (mass fraction remaining; MFR versus temperature) of NR-$PM_1$ species (OA, sulfate, nitrate, ammonium) from ACSM measurements via the TS-TD during the (a) Centreville and (b) Raleigh campaigns.

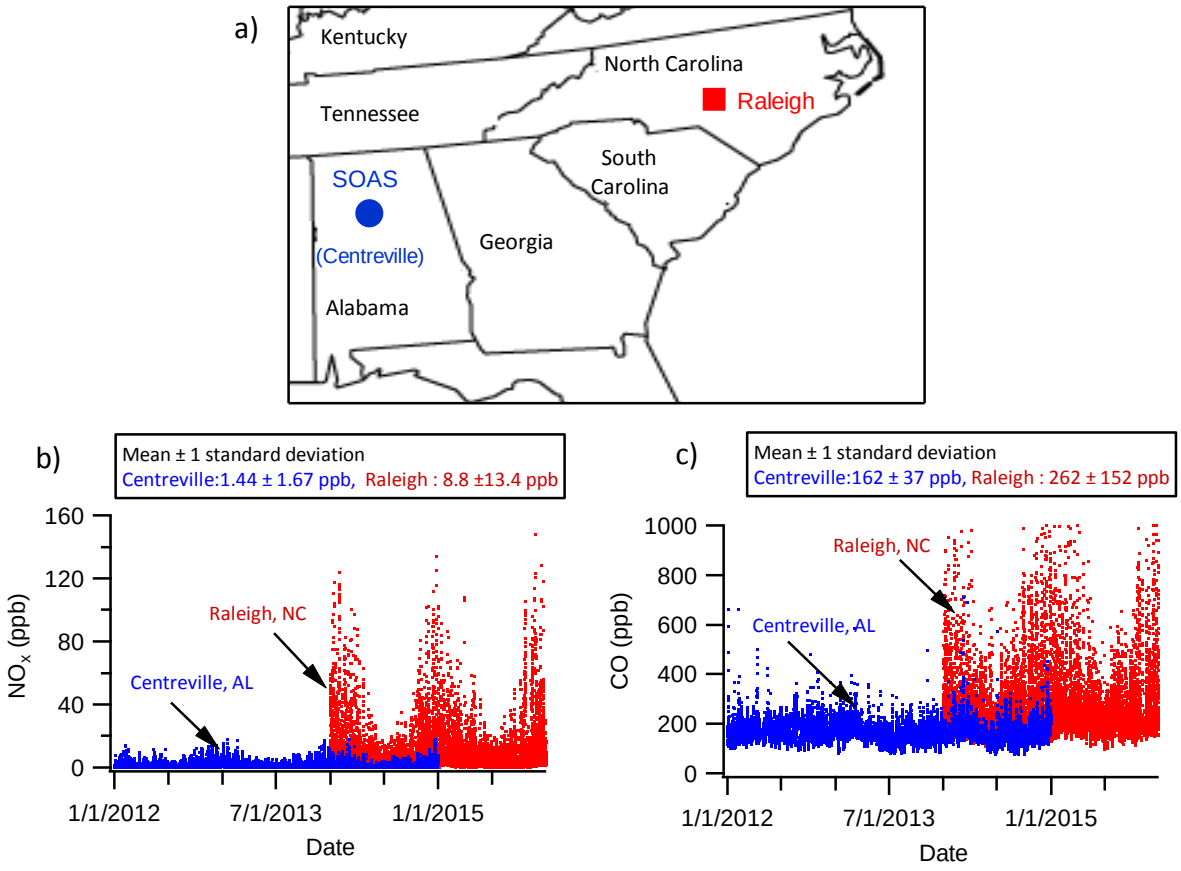


**Figure S3:** (a) Geographical locations of measurement sites and long-term trends of ambient (b) $NO_x$ and (c) CO concentrations in the study areas. Centreville data are shown from SEARCH site (atmospheric-research.com/studies/SEARCH/) at Centreville (same location of the SOAS main ground site at Centreville). Raleigh data are shown from a monitoring station at Millbrook, Raleigh (35.856 ˚N, 78.574˚W, which is ~ 12 km northeast of the NCSU measurement site) operated by North Carolina Department of Environment and Natural Resources (NC DENR).

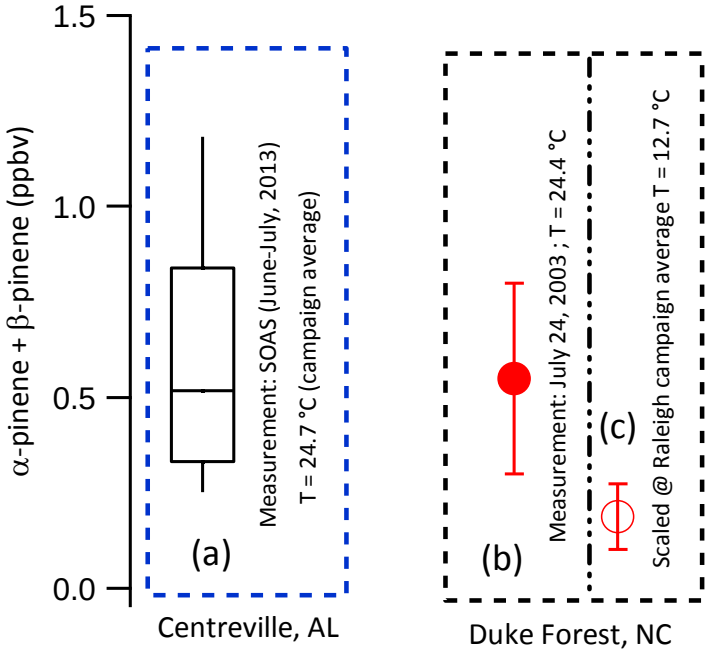


**Figure S4**: Comparison of ambient α-pinene + β-pinene concentration across two study areas. (a) Centreville data were collected during the SOAS campaign at Centreville, June-July, 2013 by Shepson's Group (Purdue University); (b) Duke Forest data were collected during CELTIC (Chemical Emission, Loss, Transformation and Interactions within Canopies) field campaign in 2003, reported from Stroud et al.(2005). Duke Forest site (35.98˚N, 79.09˚W) is about 40 km to the Northwest from the NCSU site. (c) Duke forest data are shown after scaling by a temperature adjustment factor, using the campaign- average temperature during our Raleigh measurements (October – November, 2013). The temperature adjustment factor for monoterpenes is estimated as, Ct = e0.09 (T-303), where T is in K (Warneke et al., 2010).

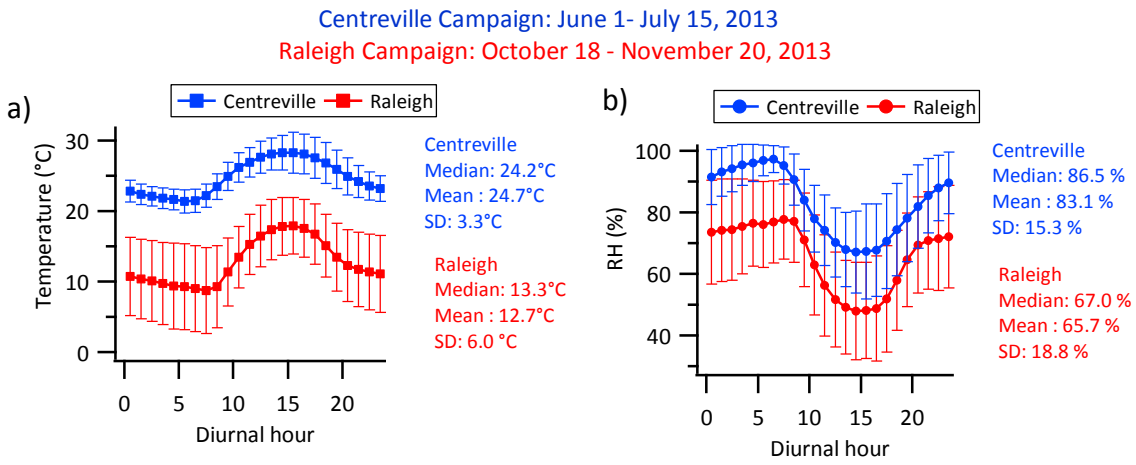


**Figure S5:** Diurnal trends of ambient temperature and relative humidity (RH) during the Centreville and Raleigh field campaign. Symbol is the mean value and error bar is ± one standard deviation of hourly data.

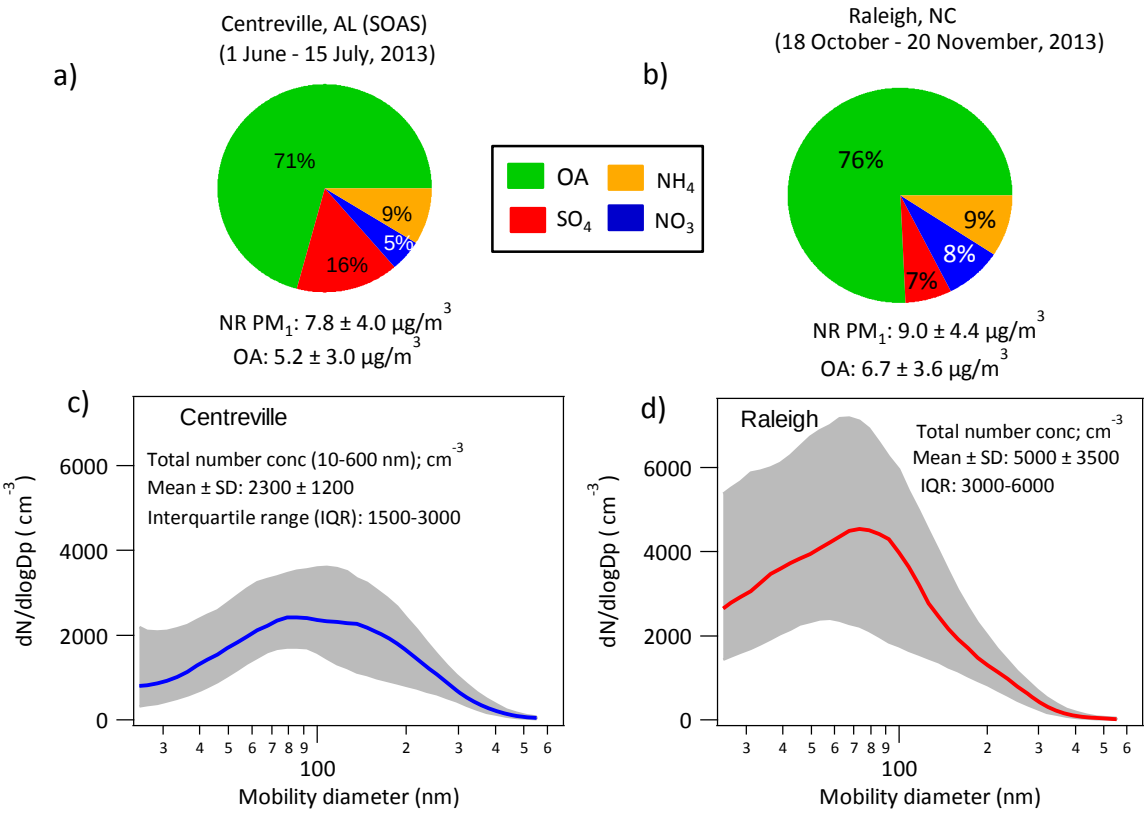


**Figure S6:** (a-b) Submicron aerosol compositions and (c-d) size distributions measured in ambient (bypass) condition. Non-refractory submicron aerosol (NR $PM_1$) composition data are measured by ACSM and number size distribution by SMPS. In panel b and c, solid lines show campaign median and shaded regions show interquartile range ($25^{th}$ to $75^{th}$ percentile). Mean ± one standard deviation (SD) of organic aerosol (OA), $PM_1$ mass concentrations, and integrated number concentrations (10-600 nm) are reported.

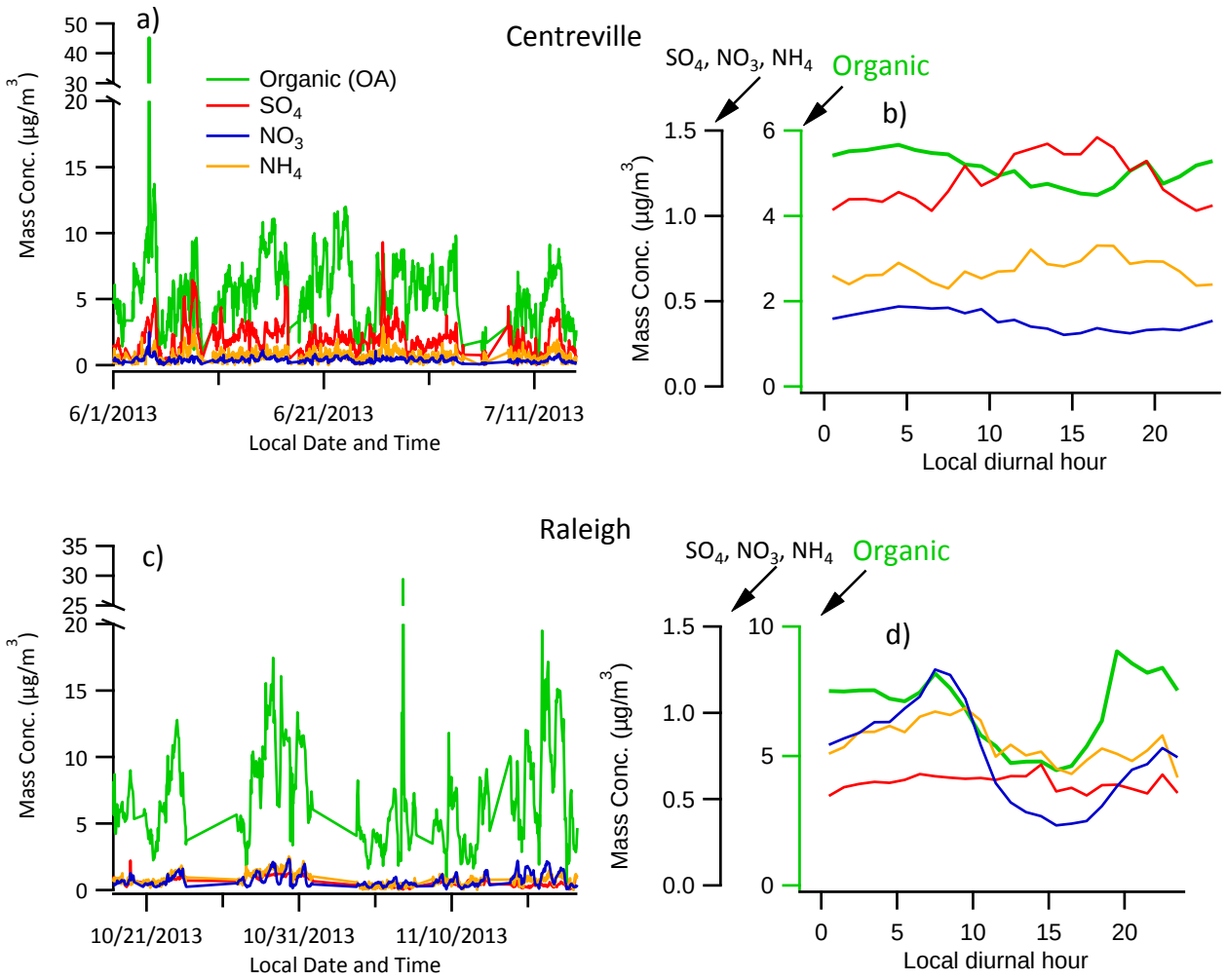


**Figure S7:** Time series and mean diurnal profiles of ambient submicron aerosol species concentrations (organics, sulfate; $SO_4$, nitrate; $NO_3$, and ammonium; $NH_4$) measured by ACSM. All ACSM data are analyzed with an assumed collection efficiency (CE) of 0.5.

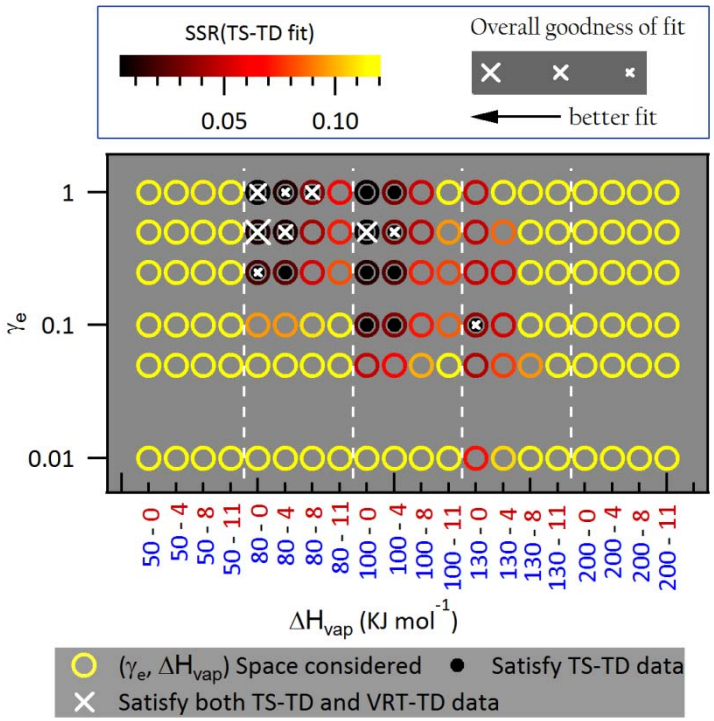


**Figure S8:** Similar to figure 3 in the main text showing analysis results for Raleigh data set. Extraction of OA gas-particle partitioning parameter ($\Delta H_{vap}$, $\gamma_e$ and $f_i$) values via evaporation kinetic model fits to campaign-average dual-TD observations. $\Delta H_{vap}$ = intercept-slope ($\log_{10}C^*$) relationship was used (e.g., 50-0 on x-axis represents intercept =50 and slope = 0). Symbols and colors represent the goodness of fit. Points with filled inner circles recreate TS-TD observations and points with a white cross (x) recreate both TD data sets to within observational variability. Crosses represent the overall goodness of fit including both TS-TD and VRT-TD observations, with larger size corresponding to a better fit.

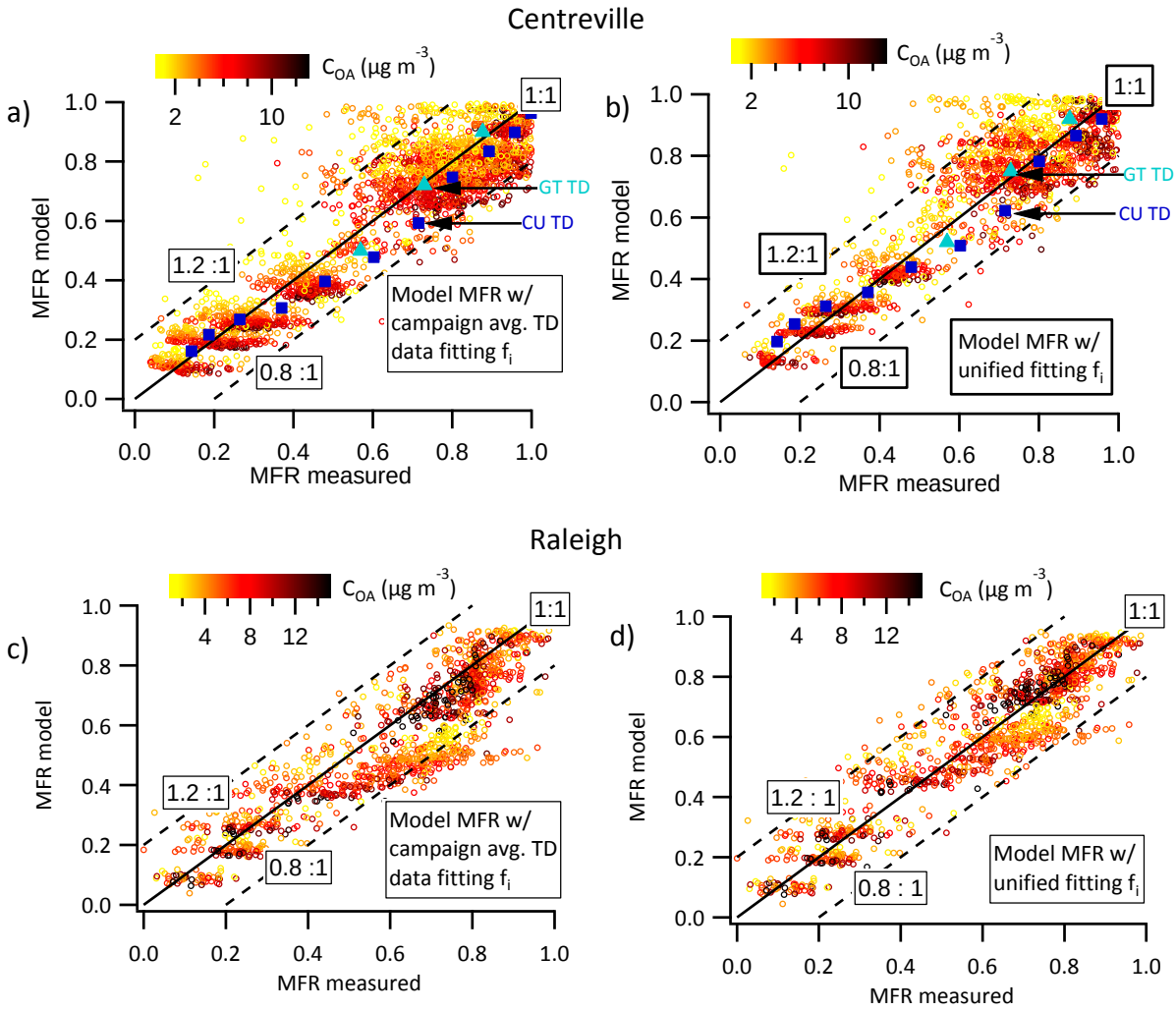


**Fig S9:** Comparison of individual observations and corresponding modeled MFRs applying the extracted $f_i$ distribution from the campaign-average fit and unified fit with $\gamma_e = 0.5$ and $\Delta H_{vap} = 100$ kj $mol^{-1}$ (see Table 1 in main text for $f_i$ distributions). (a-b) Centreville data set, (c-d) Raleigh data set. Panel a is same as Fig. 4 (a) in main text. The coefficient of determination ($r^2$) and root mean squared error (RMSE) for the panel (a) $r^2 = 0.83$; RMSE = 0.11; (b) $r^2 = 0.81$; RMSE = 0.11; (c) $r^2 = 0.82$; RMSE = 0.12; and (d) $r^2 = 0.86$; RMSE = 0.09.

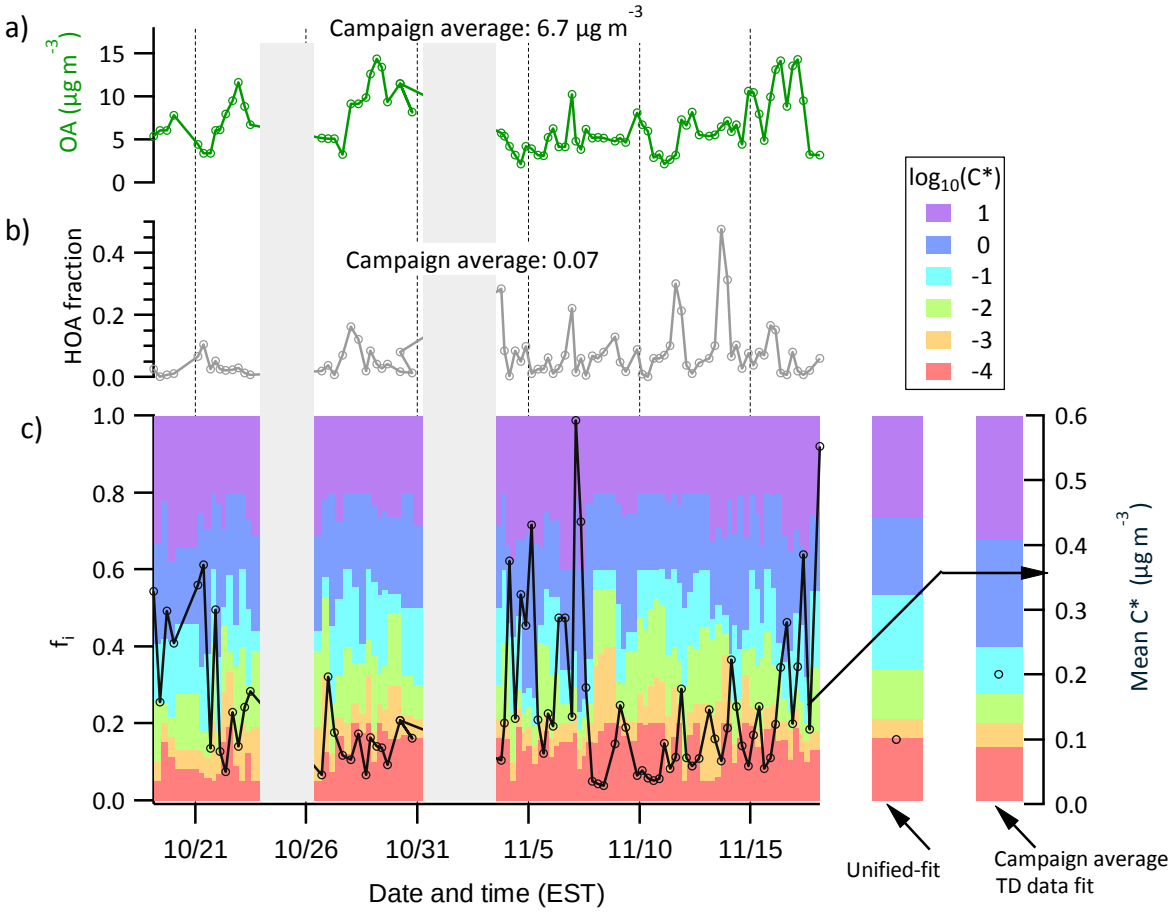


**Figure S10:** Similar to figure 6 in the main text showing analysis results for Raleigh data set. Time series of (a) ambient OA concentrations ($C_{OA}$), (b) hydrocarbon-like OA (HOA) fractional contribution to $C_{OA}$, and (c) OA volatility distribution ($f_i$) and $\overline{C^*}$ (open black circles).Tracer m/z based rough HOA are estimated as ~ 13.4 × ($C_{57}$ − 0.1 × $C_{44}$), where $C_{57}$ and $C_{44}$ are the equivalent mass concentration of tracer ion m/z 57 and 44, respectively (Ng et al., 2011b).

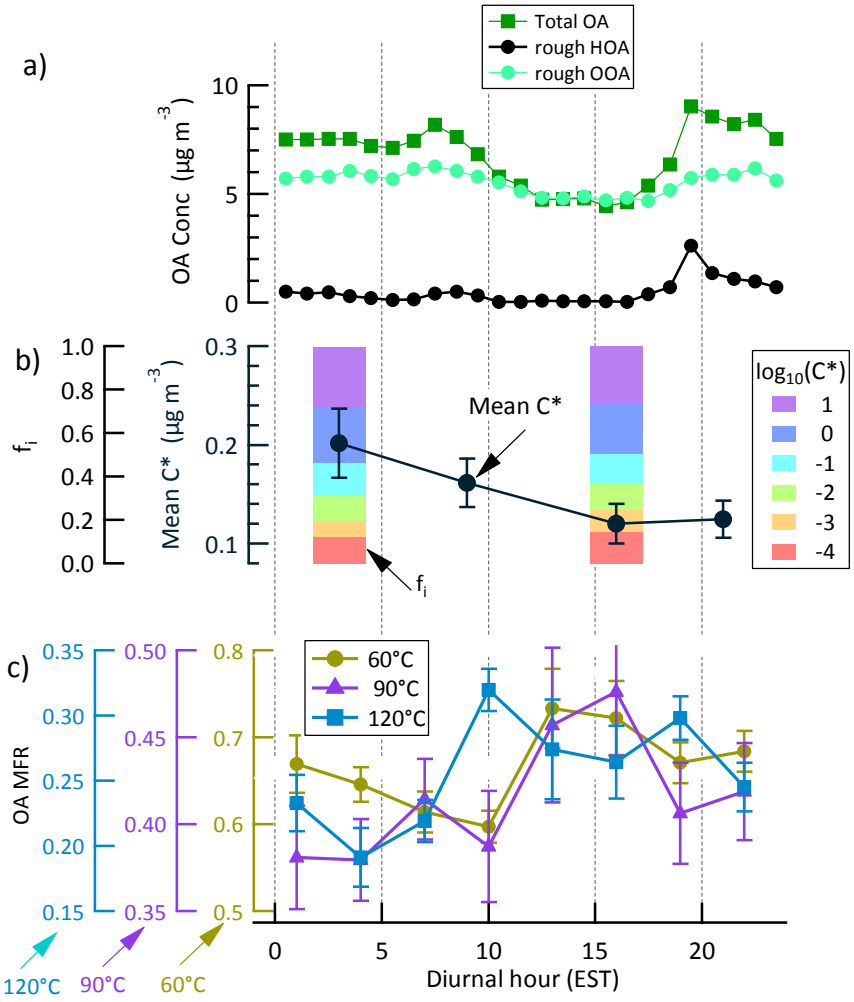


**Figure S11:** Similar to figure 7 in the main text showing analysis results for Raleigh data set. Campaign average diurnal trends of: (a) concentration of total OA and rough OA factors, (b) OA volatility ($f_i$ and $\overline{C^*}$), (c) OA MFR after heating at 60, 90 and 120 ˚C with a TD residence time of 50 s. Tracer m/z based rough OA components are estimated following Ng et al.(2011) as: hydrocarbon-like OA (HOA ~ $13.4 \times (C_{57} - 0.1 \times C_{44})$) and oxygenated OA (OOA ~ $6.6 \times C_{44}$) , where $C_{57}$ and $C_{44}$ are the equivalent mass concentration of tracer ion m/z 57 and 44, respectively.

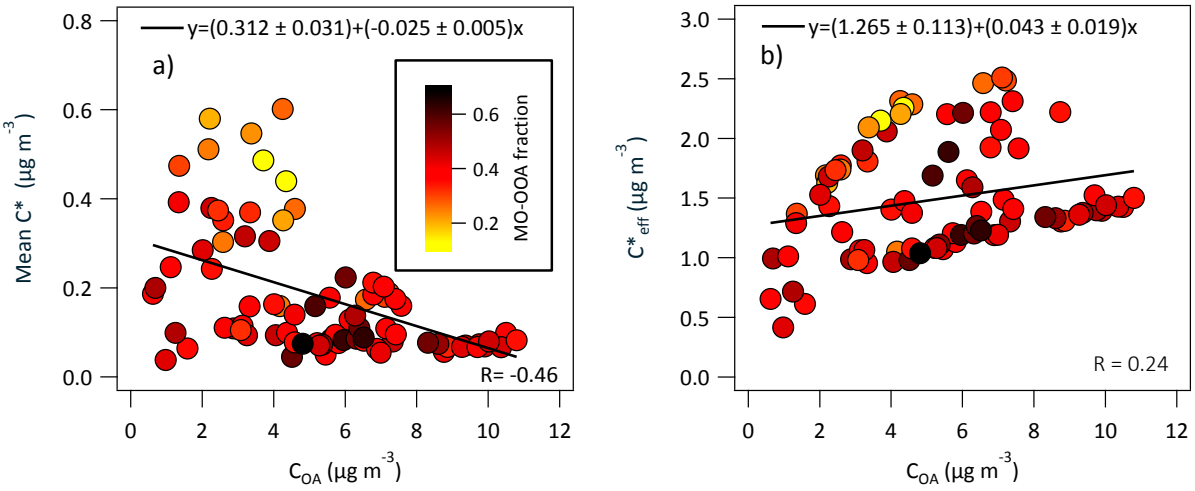


**Figure S12:** Scatter plot of (a) mean C* vs. ambient OA loading ($C_{OA}$); (b) $C^*_{eff}$ vs. ambient OA loading ($C_{OA}$). Results are shown from the Centreville campaign.

5

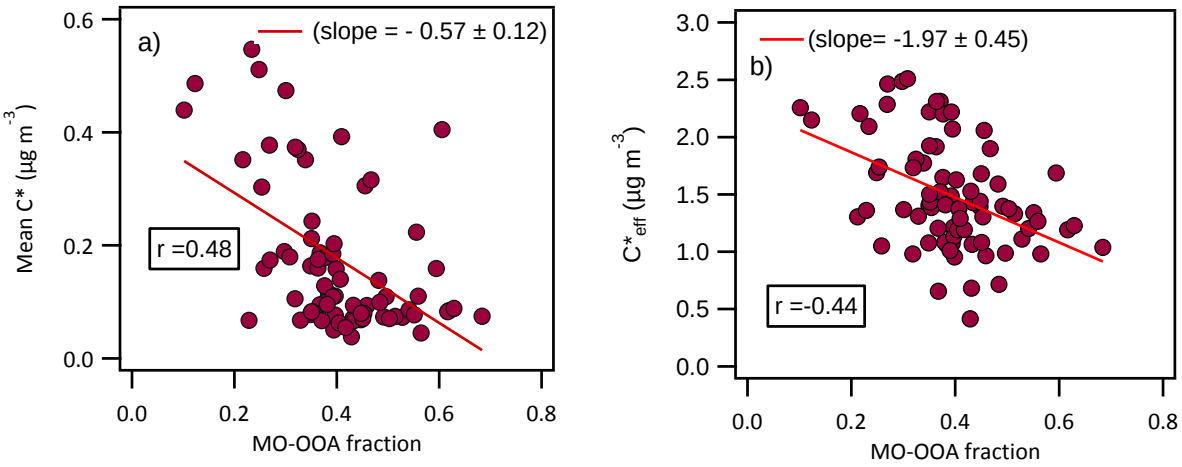


**Figure S13:** Scatter plot of (a) mean C* vs. MO-OOA fraction in $C_{OA}$; (b) $C^*_{eff}$ vs. MO-OOA fraction in $C_{OA}$. Results are shown from the

10 Centreville campaign.

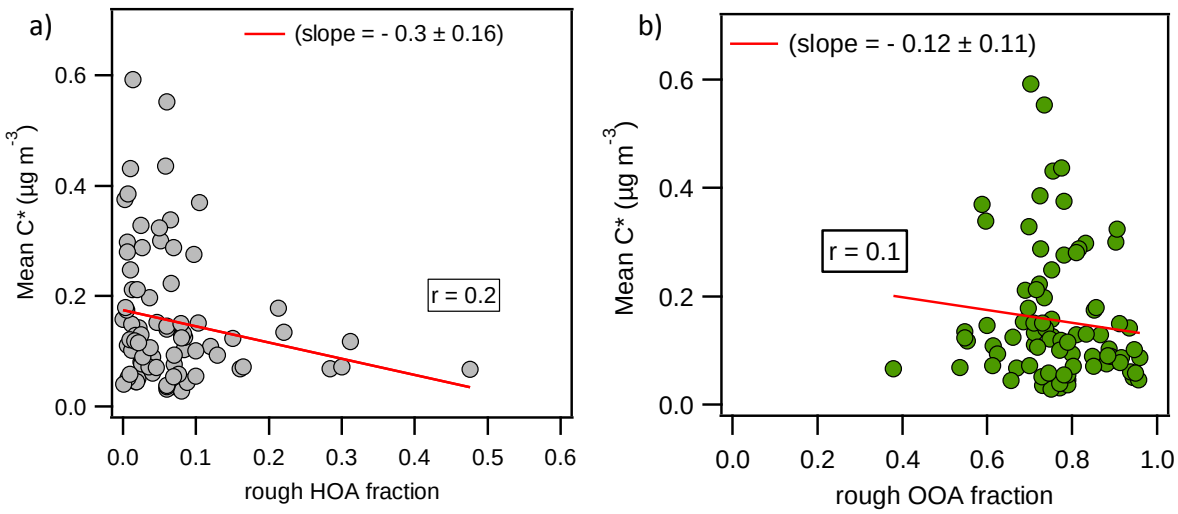


**Figure S14:** Similar to figure 8 in the main text showing analysis results for Raleigh data set. Scatter plot of mean C* verses (a) rough HOA fraction, and (b) rough OOA fraction in total OA concentration during the Raleigh campaign. For rough HOA and OOA estimation method, see Fig S11 caption.

## S4. Supplementary Tables

**Table S1:** TD kinetic model input parameters

| Parameters | Value | Notes |
|---|---|---|
| Density (kg $m^{-3}$) | 1400 | Kuwata et al., 2012 parameterization |
| Diffusion coefficient ($m^2$ $s^{-1}$) | 3.5 E-06 | Cappa and Jimenez (2010) |
| Surface tension (J $m^{-2}$) | 0.08 | Approximated as Pimelic acid, Bilde et al.(2003) |
| Molecular weight (MW) | $MW_i$ (g $mol^{-1}$) =169-28 ($\log_{10}C^*_i$) | Approximated from Di-carboxylic acid |

**Table S2:** Statistical correlation (Pearson R value) between isoprene-OA fraction to $C_{OA}$ and $f_i$'s in any particular $C^*$ bin

| $\log_{10}C^*$ bin | -4 | -3 | -2 | -1 | 0 | 10 | mean $C^*$ | $C^*_{eff}$ |
|---|---|---|---|---|---|---|---|---|
| Pearson R value | 0.02 | 0.29 | -0.07 | -0.06 | -0.14 | 0.04 | -0.06 | 0.19 |

## References


Bilde, M., Svenningsson, B., Mønster, J., and Rosenørn, T. (2003). Even−Odd Alternation of Evaporation Rates and Vapor Pressures of C3−C9 Dicarboxylic Acid Aerosols. Environ. Sci. Technol. *37*, 1371–1378.

Cappa, C.D., and Jimenez, J.L. (2010). Quantitative estimates of the volatility of ambient organic aerosol. Atmos Chem Phys *10*, 5409–5424.

Huffman, J.A., Docherty, K.S., Aiken, A.C., Cubison, M.J., Ulbrich, I.M., DeCarlo, P.F., Sueper, D., Jayne, J.T., Worsnop, D.R., Ziemann, P.J., et al. (2009). Chemically-resolved aerosol volatility measurements from two megacity field studies. Atmos Chem Phys *9*, 7161–7182.

Kuwata, M., Zorn, S.R., and Martin, S.T. (2012). Using Elemental Ratios to Predict the Density of Organic Material Composed of Carbon, Hydrogen, and Oxygen. Environ. Sci. Technol. *46*, 787–794.

Lehtinen, K., Korhonen, H., Maso, M. D. and Kulmala, M.: On the concept of condensation sink diameter, Boreal Env. Res, 8, 405–411, 2003.

Ng, N.L., Herndon, S.C., Trimborn, A., Canagaratna, M.R., Croteau, P.L., Onasch, T.B., Sueper, D., Worsnop, D.R., Zhang, Q., Sun, Y.L., et al. (2011a). An Aerosol Chemical Speciation Monitor (ACSM) for Routine Monitoring of the Composition and Mass Concentrations of Ambient Aerosol. Aerosol Sci. Technol. *45*, 780–794.

Ng, N.L., Canagaratna, M.R., Jimenez, J.L., Zhang, Q., Ulbrich, I.M., and Worsnop, D.R. (2011b). Real-Time Methods for Estimating Organic Component Mass Concentrations from Aerosol Mass Spectrometer Data. Environ. Sci. Technol. *45*, 910–916.

Saha, P.K., Khlystov, A., and Grieshop, A.P. (2015). Determining Aerosol Volatility Parameters Using a "Dual Thermodenuder" System: Application to Laboratory-Generated Organic Aerosols. Aerosol Sci. Technol. *49*, 620–632.

Stroud, C., Makar, P., Karl, T., Guenther, A., Geron, C., Turnipseed, A., Nemitz, E., Baker, B., Potosnak, M., and Fuentes, J.D. (2005). Role of canopy-scale photochemistry in modifying biogenic-atmosphere exchange of reactive terpene species: Results from the CELTIC field study. J. Geophys. Res. Atmospheres *110*, D17303.

Warneke, C., de Gouw, J.A., Del Negro, L., Brioude, J., McKeen, S., Stark, H., Kuster, W.C., Goldan, P.D., Trainer, M., Fehsenfeld, F.C., et al. (2010). Biogenic emission measurement and inventories determination of biogenic emissions in the eastern United States and Texas and comparison with biogenic emission inventories. J. Geophys. Res. Atmospheres *115*, D00F18.